USING TWO-STAGE KALMAN FILTERS AS OBSERVERS FOR SIMULTANEOUS TRAJECTORY TRACKING AND UNKNOWN INPUT ESTIMATION

Hao Deng*

Abstract

Target tracking with an unknown bias is important in the fields of navigation, trajectory determination, and so on. Kalman filter is simple in principle and widely used, however, it has poor ability for state estimation with unknown bias. To improve its performances, robust two-stage Kalman filter (RTSKF) and optimal two-stage Kalman filter (OTSKF) are adopted for target tracking and unknown bias estimation and their behaviours are compared comprehensively in this work. First, the feasibility of these filters is validated under a low-noise environment. Then, the robustness to resist the noises is investigated when the intensities of process noise and measurement noise are changed from 0.01 to 0.50. Results demonstrate the OTSKF has stronger robustness than RTSKF. Finally, the types of unknown bias are changed to test the flexibility and accuracy to track manoeuvring target.

Key Words

Target tracking, unknown bias estimation, OTSKF, RTSKF, robustness

1. Introduction

Target tracking and state estimation are important in the fields of computer vision [1], navigation [2], attitude control [3], satellite [4], track obstacles for autonomous underwater vehicle [5] and so on. For the target tracking, the accuracy is usually affected by variable factors, such as the environment disturbing, tracking methods, measurement technique, *etc.*

Target tracking is to detect the moving target and estimate the state of the target by using measurement information [6], and it usually relates to moving and multiple targets [7]. High-performance tracking can be used for accurate control and for different goals [8], such as trajectory planning [9]. For example, based on a Chebyshev pseudospectral method, Vitali *et al.* [10] proposed a multi-objective and multi-phase 4D trajectory optimisation tool to choose the best solution of an aircraft. The results obtained can satisfy the requirement of economic and environmental factors. An event-triggered attitude tracking controller was proposed by Qi *et al.* [11]. More accurate control results could be obtained. Similarly, attitude tracking synchronisation control of a space-moving target is investigated in [12]. Ziadi and Njah [13] proposed PSO-DVSF2 method to tracking moving targets for optimal motion planning approach. Based on the density-based spatial clustering of applications with noise (DBSCAN) algorithm, De *et al.* [14] proposed an adaptive localisation method for the mobile robot.

Early target tracking algorithms are mainly divided into two categories: one is based on target model modelling, and the other is based on search, such as Kalman filter [15], Winner tracker [16], Meanshift algorithm and so on [17]. The first important thing for target tracking is the accurate estimation of target state, which plays an important role in target tracking performance. Target tracking is an uncertain problem. Filtering algorithm is usually used to eliminate the related uncertainty. In practical engineering applications, the core of target tracking is filtering, and the filtering estimation results affect the accuracy of a target tracking system. Since the Kalman filter was proposed, it has been widely used and investigated [15]. For a moving target tracking, Kalman filter makes prediction based on the current states and model of the system, then it takes the measurement information to correct the estimated state. Classical Kalman filter is suitable for linear systems [18]. In practical engineering, there are many nonlinear objects, which restricts the application of Kalman filter. Therefore, many nonlinear filtering methods were proposed, such as extended Kalman filter [15], unscented Kalman filter (UKF) [19], particle filtering [20], robust Kalman filter [21] and so on. Additionally, these methods have also been developed in the field of target tracking. To realise

* Chongqing Industry Polytechnic College, Taoyuan Road 1000, Yubei District, Chongqing, China, 401120; e-mail: iaepaperei@126.com
Corresponding author: Hao Deng

Recommended by Chaomin Luo
(DOI: 10.2316/J.2024.206-0908)

real-time target tracking, Jondhale and Deshpande [22] introduced the Kalman filter and UKF into wireless sensor networks with combination of generalised regression neural network (GRNN)-based approach. They used these methods to track a two-dimensional moving target under the conditions of uncertain measurement noises. Simulation results demonstrated the favourable tracking performance of GRNN+UKF. Based on spatiotemporal context, Yang *et al.* [23] proposed a visual tracking method using Kalman filtering, which aims to improve the robustness of the target tracking process. Jung *et al.* [24] proposed an adaptive incremental backstepping controller for trajectory tracking, and this method was feasible to deal with the model uncertainties. Based on the random hypersurface model, Ma *et al.* [25] used a modified adaptive extended Kalman filter successfully to track the manoeuvring star-convex extend target. The kinematic state and shape estimation were simultaneously realised. Gu *et al.* [26] proposed an adaptive UKF for target tracking. The fading factor was adaptively changed to adjust the covariance matrix which could improve the tracking accuracy and address the divergence problem. Wang *et al.* [27] used an adaptive UKF to track a two-dimensional moving target. In this adaptive method, both the measurement noise covariance and process noise covariance were adjusted. The measurement noise covariance was adjusted by introducing a fading factor while process noise covariance was adapted by using both the innovation and the residual sequences. Zhou and Hou [28] proposed a new adaptive high-order UKF which was based on orthogonal principle and high-order UT sampling strategy. This method could solve the problem that there was obvious error using classical UKF to capture dynamic target. Another adaptive tracking method for relative state estimation of a non-cooperative target was proposed by Yin *et al.* [29]. In this method, a current statistical jerk model-based extended Kalman filter was improved by interacting multiple model algorithm. It can be used to track non-cooperative spacecraft with continuous-thrust manoeuvres. Liang *et al.* [30] developed a distributed Kalman filtering technique with trust-based dynamic combination strategy, which can improve resilience against cyber-attacks.

While there is an unknown bias as input, successful estimation of the input estimation is useful for system tracking and control. Simultaneous target tracking and unknown bias estimation using Kalman filter have been focused on in recent years. Though different methods based on Kalman filter were developed, they mainly focused on the state estimation, which was used for target tracking. For the simultaneous estimation of state and unknown input, Ji *et al.* [31] proposed an input estimation method, which combined Kalman filter with recursive least-squares algorithm, and they used this method to estimate the thermal state and input of a thermal system. However, there would be extreme fluctuation in the initial period for the unknown input estimation [32]. This phenomenon has been illustrated in the state estimation of thermal systems [33]. Wang *et al.* introduced fuzzy inference into this method and adaptively adjust the process noise covariance in the heat source estimation of instantaneous heat transfer system [34] and state monitoring of absorber tube [35]. Though this method improved the performances of input estimation and state estimation, the membership function and universe should be determined when the fuzzy inference method is used. These two factors are depended on the study object. And there is not a universal rule to determine these factors. Another possible way is to regard the unknown input bias as an augmented state in Kalman filter. This increases the dimension of the state vector to the total dimension of state and input. However, it leads to a significant increase in the dimension of the state transform matrix, making the calculation complex. To overcome this problem, a two-stage Kalman filter method was proposed. That is, one Kalman filter is used for state estimation while another one is used for unknown input estimation. To obtain optimal estimation of unknown input in the mean square error sense, an optimal two-stage Kalman filter (OTSKF) was derived [36]. And it has been applied in cyber-attack detection [37]. In order to avoid the effect of unknown inputs, the blending matrix and the bias filter in OTSKF are modified to obtain a robust two-stage Kalman filter (RTSKF) [38]. The OTSKF has been used for simultaneous state and cyberattack estimation in automatic generation control [39]. Related two-stage Kalman filter has been widely developed for power system state estimation [40].

Though the Kalman filter methods were proposed for state estimation, there is a few work focussing on the comparative investigation of different Kalman filter methods, especially in the fields of manoeuvring target tracking. As manoeuvring target has high uncertainty, its trajectory tracking and state estimation are quite complex problems. To investigate the comprehensively comparison of the performances of RTSKF and OTSKF, the effects of different noises and unknown inputs were studied to test the abilities of target tracking and unknown bias estimation. The comparison between the performances of OTSKF and RTSKF for manoeuvring target tracking is the main topic in this work, instead of the manoeuvring target modelling. Results demonstrated the feasibilities of these methods in the tracking of manoeuvring target and gave a guide for the choosing of estimation methods under different conditions.

2. Model of a Manoeuvring Target

In the modern control theory, a dynamic system can be described by the state-space model, which contains the state equation and observation equation. Consider the linear discrete stochastic system with unknown bias in the following form,

$$x_{k+1} = A_k x_k + E_k d_k + w_k \tag{1}$$

$$d_{k+1} = d_k + w_k^d \tag{2}$$

$$y_k = H_k x_k + \eta_k \tag{3}$$

where, $x_k \in R^n$ is the state vector of the system; $d_k \in R^P$ is the unknown bias which is the input of this linear discrete system; y_k is the measurement vector. A_k, E_k and H_k are state transform matrix, input matrix and measurement

Table 1
Acceleration Sequence in this Section

Time (s)	1–30	31–45	46–55	56–80	81–98	99–119	120–139	140–150	151–160
$[a_x, a_y]$	[0,0]	[8,22]	[12], [27]	$[0, 0]$	[15,2]	$[-2, 9]$	$[0, -1]$	$[28, -1]$	$[0, 0]$

matrix, respectively. The w_k, w_k^d and η_k are independent noise sequence with the covariances: $E\{w_k w_l'\} = Q_k$, $E\{\eta_k \eta_l'\} = R_k$, and $E\{w_k^d (w_l^d)'\} = Q_k^d$. Equation (1) is the state equation and (2) describes the input information of the linear discrete system. Equation (3) is the observation equation.

Manoeuvre estimation is a significant problem in target tracking, especially with an unknown bias. It is quite a difficult problem due to its high uncertainty. In the kinematic model, a manoeuvre is always modelled using its acceleration variations, which has a similar form with a linear discrete stochastic system model. A manoeuvring target model on $(x,\ y)$ coordinate plane is described as follows:

$$x_{k+1} = Ax_k + E(a_k + \widetilde{a}_k) \tag{4}$$
$$z_k = Hx_k + v_k \tag{5}$$

where, $x = [x, V_x, y, V_y]^T$ is the state vector consisting of position coordinate and velocity in each direction; $a = [a_x, a_y]^T$ is the acceleration vector, which is an unknown bias. $\widetilde{a}$ and $\boldsymbol{v}$ are independent acceleration and measurement noise vectors, which consists of Gaussian white noise. Equation (4) is the state equation and (5) is the observation equation used in this work. The covariance matrixes of $\widetilde{a}$ and $\boldsymbol{v}$ are $\boldsymbol{Q}$ and $\boldsymbol{R}$. According to the movement equation,

$$A = \begin{bmatrix} 1 & T & 0 & 0 \\ 0 & 1 & 0 & 0 \\ 0 & 0 & 1 & T \\ 0 & 0 & 0 & 1 \end{bmatrix}, E = \begin{bmatrix} T^2/2 & 0 \\ T & 0 \\ 0 & T^2/2 \\ 0 & T \end{bmatrix}, H = \begin{bmatrix} 1 & 0 & 0 & 0 \\ 0 & 0 & 1 & 0 \end{bmatrix}$$

where, T is a discrete time step.

As a term in state equation, the term $\boldsymbol{a}$ is the input of the system, which is also the acceleration vector. In this paper, the input data $\boldsymbol{a}$ is referenced from the literature [41], which was used to test the feasibility of a target tracking method. The acceleration vector, namely, the input data $\boldsymbol{a}$ consists of two elements, which are the acceleration components in x and y directions. In this work, the initial position is set on the (0,0) and the initial velocity is zero. The acceleration vector is chosen as Table 1.

It is seen that the input data series serves to evaluate algorithms' peak errors, steady-state errors, and response times.

3. Methodology of Two-stage Kalman Filters

There have been many works focussing on the state estimation of two-dimensional moving object using Kalman filter [42]. In this work, the OTSKF and RTSKF are used to track a manoeuvring target which moves on a two-dimensional plane. The main objective of this work is to compare the performances of OTSKF and RTSKF for manoeuvring target tracking. As these two methods have been derived in previous works, they are clearly given in this section.

3.1 Robust Two-stage Kalman Filter

Hsieh [38] proposed an RTSKF, which can be used to estimate the state of linear system without effects by unknown inputs. The RTSKF for simultaneous estimation of unknown input and state can be described by the following equations [38]:

$$\widehat{x}_{k/k} = \overline{x}_{k/k} + V_k \widehat{d}_{k/k} \tag{6}$$
$$\widehat{P}^x_{k/k} = \overline{P}^x_{k/k} + V_{k/k} P^d_{k/k} V'_{k/k} \tag{7}$$

where, $\widehat{x}_{k/k}$ is the optimal estimation of the system state, namely the posterior estimation; $\widehat{d}_{k/k}$ is the optimal estimation result of the unknown input; $\boldsymbol{V_k}$ is the gain matrix to obtain the optimal state; $\widehat{P}_{k/k}$ is the estimation error covariance of the state. The $\overline{x}_{k/k}$ is given by

$$\overline{x}_{k/k-1} = A_{k-1} \widehat{x}_{k-1/k-1} \tag{8}$$
$$\overline{x}_{k/k} = \overline{x}_{k/k-1} + K^{\overline{x}}_k (y_k - H_k \overline{x}_{k/k-1}) \tag{9}$$
$$\overline{P}^x_{k/k-1} = A_{k-1} \widehat{P}^x_{k-1/k-1} A'_{k-1} + Q_{k-1} \tag{10}$$
$$K^{\overline{x}}_k = \overline{P}^x_{k/k-1} H'_k C^{-1}_k \tag{11}$$
$$\overline{P}^x_{k/k} = (I - K^{\overline{x}}_k H_k) \overline{P}^x_{k/k-1} \tag{12}$$

where, $K^{\overline{x}}_k$ is the gain matrix to correct the state estimation; $\boldsymbol{I}$ is a unit matrix; and $\boldsymbol{y_k}$ is the observation result.

The optimal estimation result of the unknown input $\widehat{d}_{k/k}$ can be obtained using the following equations:

$$\widehat{d}_{k/k} = K^d_k (y_k - H_k \overline{x}_{k/k-1}) \tag{13}$$
$$K^d_k = P^d_{k/k} E'_{k-1} H'_k C^{-1}_k \tag{14}$$
$$P^d_{k/k} = \{E'_{k-1} H'_k C^{-1}_k H_k E_{k-1}\}^{-1} \tag{15}$$

where, K^d_k is the gain matrix to obtain the optimal estimation of the input vector. $\mathbf{V}_k$ and $\mathbf{C}_k$ are obtained as follows,

$$V_k = (I - K^{\overline{x}}_k H_k) E_{k-1} \tag{16}$$
$$C_k = H_k \overline{P}^x_{k/k-1} H'_k + R_k \tag{17}$$

3.2 Optimal Two-stage Kalman Filter

As for the linear discrete model described by (1)–(3), the $\widehat{d}_{k/k}$ is an optimal filter of the unknown inputs in the mean

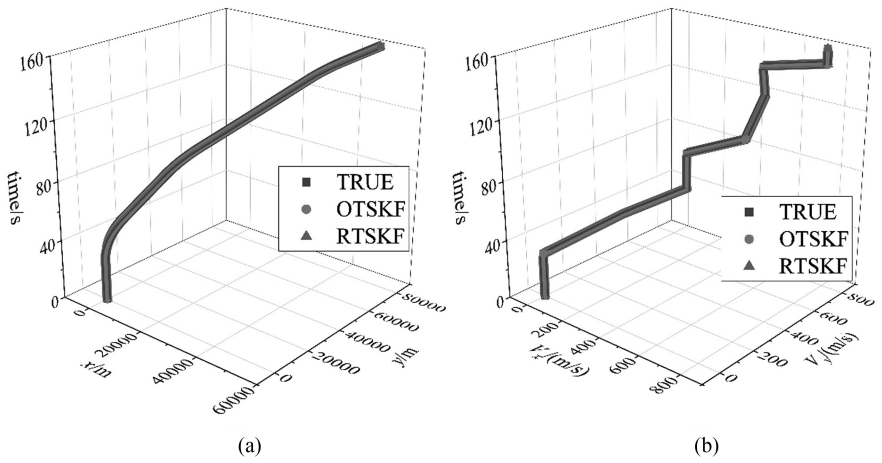

Figure 1. Manoeuvring target tracking results using OTSKF and RTSKF: (a) trajectory of manoeuvring target and (b) velocity estimation result.

square error sense. The optimal estimation equation for state and its estimation error covariance matrix should be as follows:

$$\widehat{x}_{k+1/k+1} = \widetilde{x}_{k+1/k+1} + \beta_{k+1/k+1}\widehat{d}_{k+1/k+1} \quad (18)$$

$$P^x_{k+1/k+1} = \widetilde{P}^x_{k+1/k+1} + \beta_{k+1/k+1}P^b_{k+1/k+1}\beta'_{k+1/k+1} \quad (19)$$

where, $\widehat{x}_{k+1/k+1}$ and $\widehat{d}_{k+1/k+1}$ are the optimal estimation results of state and unknown input; $P^x_{k+1/k+1}$ is the estimation error covariance of the state; $\beta_{k+1/k+1}$ is the coupling term in the following coupling equation.

The optimal estimation of state vector is obtained by updating the state estimation result without input formation using the estimated optimal input. The state estimator is solved using the following equations:

$$\widetilde{x}_{k+1/k+1} = \widetilde{x}_{k+1/k} + \widetilde{K}^x_{k+1}\widetilde{\gamma}_{k+1} \quad (20)$$

$$\widetilde{P}^x_{k+1/k+1} = (I - \widetilde{K}^x_{k+1}H_k)\widetilde{P}^x_{k+1/k} \quad (21)$$

$$\widetilde{K}^x_{k+1} = \widetilde{P}^x_{k+1/k}H'_k(\widetilde{G}_{k+1})^{-1} \quad (22)$$

$$\widetilde{G}_{k+1} = H_k\widetilde{P}^x_{k+1/k}H'_k + R_k \quad (23)$$

$$\widetilde{\gamma}_{k+1} = y_{k+1} - H_k\widetilde{x}_{k+1/k} \quad (24)$$

$$\widetilde{x}_{k+1/k} = A_{\,\mathrm{k}}\widetilde{x}_{k/k} + \vartheta_k\widehat{d}_{k/k} - \beta_{k+1/k}\widehat{d}_{k+1/k} \quad (25)$$

$$\widetilde{P}^x_{k+1/k} = A\widetilde{P}^x_{k/k}A' + Q_k + \vartheta_k P^b_{k/k}\vartheta'_k - \beta_{k+1/k}P^b_{k+1/k}\beta'_{k+1/k} \quad (26)$$

where, $\widetilde{x}_{k+1/k+1}$ is the posterior state estimation corrected by measurement information; $\widetilde{x}_{k+1/k}$ is the priori state estimation; ϑ_k is the coupling equation described in the following part. $\widehat{d}_{k/k}$ is obtained using the following equations:

$$\widehat{d}_{k+1/k+1} = \widehat{d}_{k/k} + K^b_{k+1}\gamma_{k+1} \quad (27)$$

$$P^b_{k+1/k+1} = (I - K^b_{k+1}L_{k+1/k})P^b_{k+1/k} \quad (28)$$

$$K^b_{k+1} = P^b_{k+1/k}L'_{k+1/k}(L_{k+1/k}P^b_{k+1/k}L'_{k+1/k} + \widetilde{G}_{k+1})^{-1} \quad (29)$$

$$\gamma_{k+1} = \widetilde{\gamma}_{k+1} - L_{k+1/k}\widehat{d}_{k/k} \quad (30)$$

$$P^b_{k+1/k} = P^b_{k/k} + Q^d_k \quad (31)$$

where, $P^b_{k+1/k}$ is the priori estimation error covariance of the input; $P^b_{k+1/k+1}$ is the posterior estimation error covariance of the input. And the coupling equations $\beta_{k+1/k+1}$, ϑ_k, and $L_{k+1/k}$are given as follows:

$$\beta_{k+1/k+1} = \beta_{k+1/k} - \widetilde{K}^x_{k+1}L_{k+1/k} \quad (32)$$

$$L_{k+1/k} = H_k\beta_{k+1/k} \quad (33)$$

$$\beta_{k+1/k} = \vartheta_k P^b_{k/k}(P^b_{k+1/k})^{-1} \quad (34)$$

$$\vartheta_k = A_k\beta_{k/k} + E_k \quad (35)$$

4. Performance Evaluation of RTSKF and OTSKF

In this section, abovementioned two methods, namely, RTSKF and OTSKF are applied to track a manoeuvring target and estimate the unknown bias simultaneously.

4.1 Feasibility of RTSKF and OTSKF for Target Tracking and Unknown Bias Estimation

To validate the feasibility of RTSKF and OTSKF, the model in Section 3 is chosen as the manoeuvring target. Initial guesses of state vector and unknown bias are assumed as zero vectors. When $\boldsymbol{Q}$ and $\boldsymbol{R}$ are set as $0.001\boldsymbol{I}$ and $0.001\boldsymbol{I}$, the manoeuvring target results are shown in Fig. 1.

The target position changes over time. It is seen that during this process the trajectory of this target has variable curvature in different periods. During the first 30 s, the position keeps as (0, 0) due to zero acceleration. At the final second, the true position of the target is (49,673.37 m, 81,616.12 m) while the tracked ones using OTSKF and RTSKF are (49,673.33 m, 81,615.94 m) and (49,673.37 m, 81,616.11 m). The tracking error is very low and the tracked trajectory of this manoeuvring target using OTSKF or RTSKF agrees with the true trajectory accurately. The estimated velocity vectors and true velocity vector are (776.00 m/s, 794.00 m/s). And the estimated velocity change curves in Fig. 1(b) coincide with the true

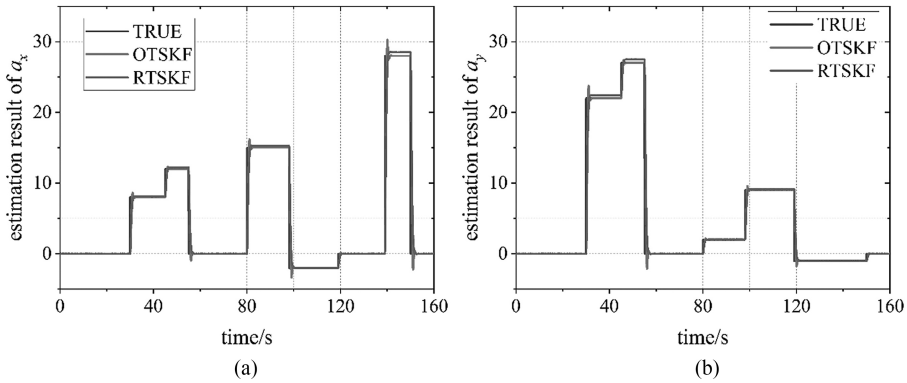

Figure 2. Estimation results of the unknown bias: (a) a_x and (b) a_y.

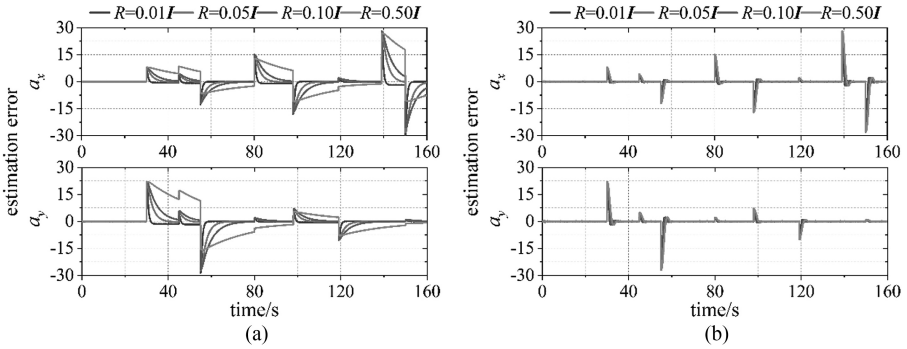

Figure 3. Effects of measurement noise on acceleration estimation: (a) RTSKF and (b) OTSKF.

value. Therefore, both the RTSKF and OTSKF can be used for the state estimation of the manoeuvring target. The estimation results of the unknown bias, namely the acceleration sequence, are shown in Fig. 2.

In the initial period, there is no difference between the true value and the estimated value due to the reason that initial guess value is the same as the true acceleration sequence. When there is a change of a_x or a_y, the estimated result can quickly track the true value. It is clearly exhibited that after the moment of sudden change, there is a slight overshoot of the estimated bias using OTSKF. However, it disappears in a very short period. For the RTSKF, the estimated bias matches with the changes of true value. In some periods, estimated results are slightly higher than true value. The accuracy of these tracking methods is high enough for the unknown bias estimation. Comprehensively considering the state and bias estimation, the OTSKF and RTSKF are feasible for target tracking and unknown bias estimation.

4.2 Effects of Variable R on RTSKF and OTSKF

It is unavoidable that there are noises in observation, which is affected by environmental noise, sensor and so on. When the covariance of measurement noises is changed as $0.01\boldsymbol{I}$, $0.05\boldsymbol{I}$, $0.10\boldsymbol{I}$ and $0.50\boldsymbol{I}$, the estimation results of the unknown acceleration sequence using RTSKF and OTSKF are shown in Fig. 3. In these cases, the $\boldsymbol{Q}$ keeps constant as $0.001\boldsymbol{I}$.

When the unknown bias is zero, there is no difference between the estimation results using RTSKF and OTSKF. Once the acceleration changes, an obvious error occurs in the estimation error of a_x or a_y no matter whether the RTSKF or OTSKF is used for bias estimation. For RTSKF, when $\boldsymbol{R} = 0.01\boldsymbol{I}$, the sudden changes of estimation error can be eliminated in 2∼3 s. With the increase of intensity of measurement noise, the time to high-accuracy estimation becomes longer. When $\boldsymbol{R}$ rises to $0.50\boldsymbol{I}$, the estimation error of unknown a_x or a_y cannot reach zero. It can only reflect the changing trend of the acceleration bias, which means the estimation of unknown bias failed under this condition. For OTSKF, it is similar to RTSKF that there is an error when acceleration changes sharply. The error of OTSKF is of same level as that of RTSKF at the same moment. The difference is that the time to recover zero is very short for OTSKF. It is seen that the time to recover zero becomes longer when the $\boldsymbol{R}$ increases, which is similar to RTSKF. Due to its fast-tracking ability, the error can be eliminated in a short period even $\boldsymbol{R} = 0.50\boldsymbol{I}$. Therefore, the estimation ability for unknown bias using OTSKF can resist the higher intensity of measurement noise than RTSKF. The state estimation results are shown in Fig. 4.

The tracking error of trajectory mainly occurs at the moment of acceleration change. And it recovers to zero due to the tracking ability of the two methods. The tracking error becomes larger when the intensity of measurement noise increases. For RTSKF, when $\boldsymbol{R}$ increases from $0.01\boldsymbol{I}$ to $0.50\boldsymbol{I}$, the estimation errors of x vary in the ranges of

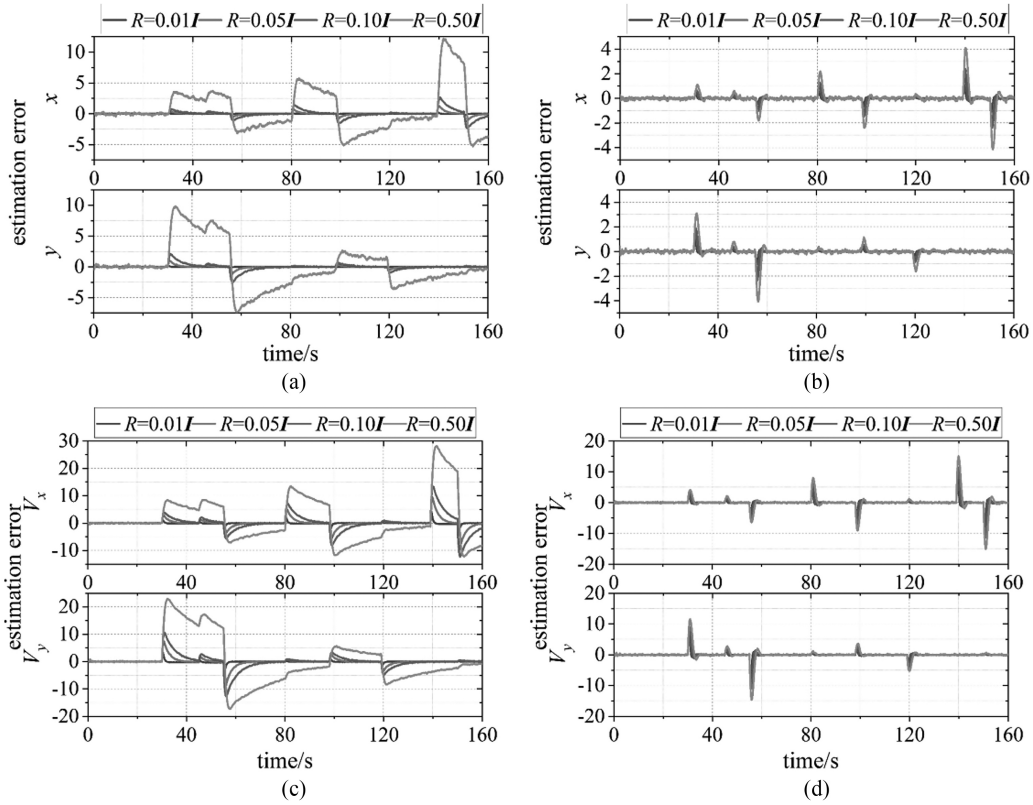

Figure 4. Effects of measurement noise on state estimation results: (a) error of trajectory using RTSKF; (b) error of trajectory using OTSKF; (c) error of velocity using RTSKF; and (d) error of velocity using OTSKF.

[−0.26 m, 0.25 m], [−1.31 m, 1.26 m], [−2.31 m, 2.64 m] and [−5.32 m, 12.20 m] while the estimation error of y distribute in the ranges of [−0.24 m, 0.19 m], [−1.24 m, 1.00 m], [−2.47 m, 2.09 m] and [−7.44 m, 9.86 m]. The maximum error of the x position occurs near 140 s due to the large variation of a_x. The maximum error of the y position occurs after the 30 s. Except for the condition of $\boldsymbol{R} = 0.50\boldsymbol{I}$, the estimation error of trajectory can recover to zero after a sudden change of acceleration. For OTSKF, the estimation error of trajectory is different from that of RTSKF under the same condition. when $\boldsymbol{R}$ increases from $0.01\boldsymbol{I}$ to $0.50\boldsymbol{I}$, the estimation errors of x vary in the ranges of [−1.10 m, 1.10 m], [−1.91 m, 1.89 m], [−2.40 m, 2.41 m] and [−4.16 m, 4.10 m] while the estimation error of y distributes in the ranges of [−1.06 m, 0.86 m], [−1.84 m, 1.49 m], [−2.34 m, 1.88 m] and [−4.07 m, 3.12 m]. It is seen that when $\boldsymbol{R}$ is less than $0.10\boldsymbol{I}$, the trajectory estimation error range of RTSKF is narrower than that of OTSKF. They have similar accuracy when the $\boldsymbol{R} = 0.10\boldsymbol{I}$. When the intensity of measurement noise increases further, the OTSKF has a more favourable performance than RTSKF. However, it should be noted that the OTSKF has faster tracking ability, which can eliminate the estimation error quickly. For this reason, the global error of OTSKF is lower than that of RTSKF under all conditions. As for the estimation of the velocity of the manoeuvring target, the performance is similar with the estimation results of position. The estimation error increases with the climbing of measurement noise. And OTSKF shows more favourable performance than RTSKF in all conditions due to the reason that OTSKF shows fast tracking ability and strong robustness to resist the measurement noise.

4.3 Effects of Variable Q on RTSKF and OTSKF

In the movement of a manoeuvring target, the model error or bias noise is always reflected by the variable $\boldsymbol{Q}$ in the state-space equation. When the $\boldsymbol{R}$ keeps constant as $0.001\boldsymbol{I}$, the covariance of bias noises $\boldsymbol{Q}$ is changed as $0.01\boldsymbol{I}$, $0.05\boldsymbol{I}$, $0.10\boldsymbol{I}$ and $0.50\boldsymbol{I}$. Under these conditions, the estimation results of unknown acceleration sequences using RTSKF and OTSKF are shown in Fig. 5.

For RTSKF, the estimation error of unknown bias increases with the climbing of $\boldsymbol{Q}$. The estimation result of RTSKF under the condition of $\boldsymbol{Q} = 0.50\boldsymbol{I}$ is definitely unbelievable. Under other conditions, the estimation error of acceleration can reflect the variations of true value and the estimation error tends to recover after the sudden changes in acceleration sequence. However, due to its poor tracking ability, the estimation performance deteriorates when $\boldsymbol{Q} = 0.10\boldsymbol{I}$. Under the conditions of $\boldsymbol{Q} = 0.01\boldsymbol{I}$ and $0.05\boldsymbol{I}$, the estimation error can reach zero in most of the periods. The maximum error is always related to the sharp change of acceleration. Different from RTSKF, the estimation of acceleration using OTSKF is of high accuracy. Though there is error at the moment of a sudden change of unknown bias, the error can be zero in next several steps. This is much better than that of RTSKF. Compared with previous results, it can be found that the higher $\boldsymbol{Q}$ can accelerate the tracking process of unknown bias. This

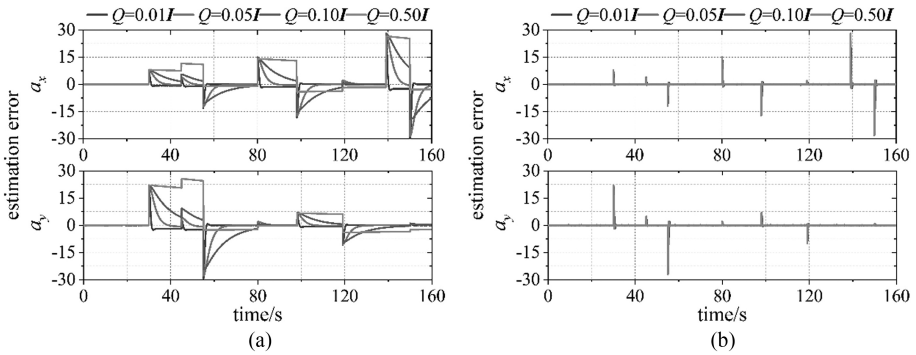

Figure 5. Effects of $\boldsymbol{Q}$ on the estimation of unknown acceleration: (a) RTSKF and (b) OTSKF.

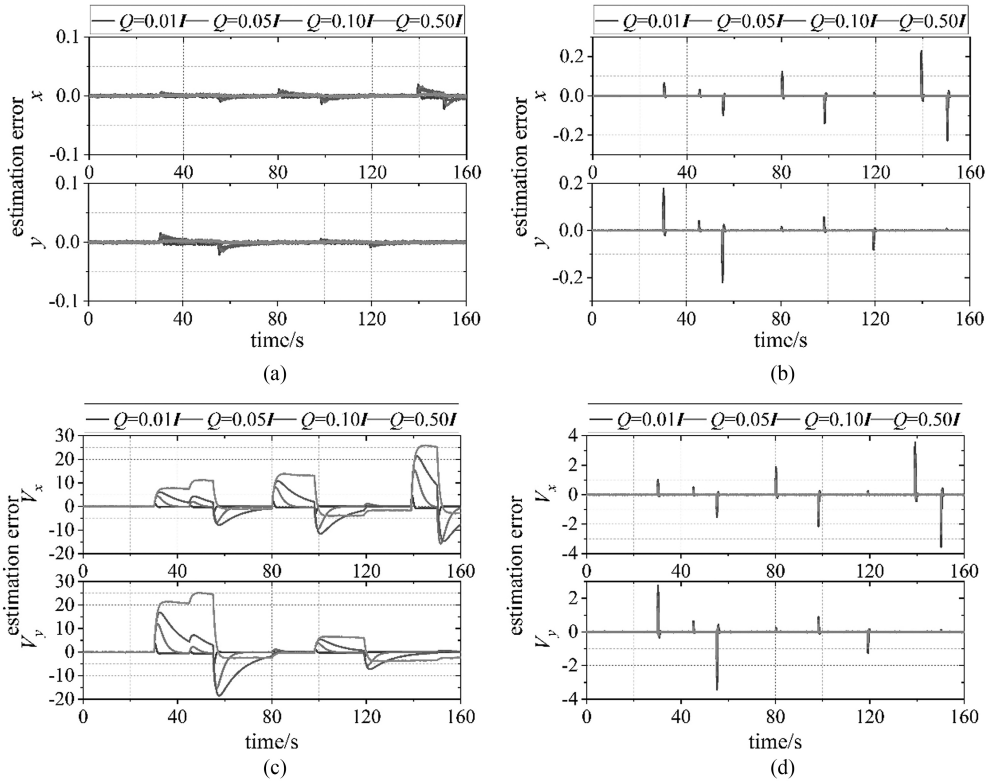

Figure 6. Effects of $\boldsymbol{Q}$ on state estimation results: (a) error of trajectory using RTSKF; (b) error of trajectory using OTSKF; (c) error of velocity using RTSKF; and (d) error of velocity using OTSKF.

is also demonstrated in Fig. 5(b). The estimation error can reach zero earlier when $\boldsymbol{Q}$ is larger. The reason for this phenomenon is that $\boldsymbol{Q}$ plays an important role to determine the gain $\boldsymbol{Kb}$ which is used to adjust the bias estimation. When $\boldsymbol{Q}$ increases, the $\boldsymbol{Kb}$ also increases to a relatively stable value within a shorter period. Therefore, proper increasing of $\boldsymbol{Q}$ can improve the tracking ability of OTSKF. On the contrary, increasing $\boldsymbol{Q}$ leads to the decrease in gain for correcting bias estimation in RTSKF, which deteriorates the estimation result. In these cases, the state estimation results using RTSKF and OTSKF are shown in Fig. 6.

What differs from the unknown bias estimation results is that the position estimation result using RTSKF is quite favourable. It is seen that under different conditions, the estimation error of coordinate of the manoeuvring target is lower than 0.05 m while RTSKF is employed. When there is a sudden change in acceleration sequence, the position estimation can keep an accurate performance with slight fluctuation. While the $\boldsymbol{Q}$ increases, the estimation error of coordinate becomes lower. For OTSKF, it also shows good performance for the trajectory tracking. There is only a small fluctuation at the moment when the acceleration changes. Its recovery time is shorter than that of RTSKF. Additionally, it can be found in Fig. 6(b) that the fluctuation intensity at the sudden change moment of acceleration becomes lower when $\boldsymbol{Q}$ rises to a higher level. This is similar to the trajectory tracking result using RTSKF. However, for the velocity estimation, the RTSKF shows unsatisfactory accuracy. when $\boldsymbol{Q}$ increases from $0.01\boldsymbol{I}$ to $0.50\boldsymbol{I}$, the estimation errors of V_x vary in the ranges of [−5.30 m/s, 4.66 m/s], [−15.80 m/s, 15.32

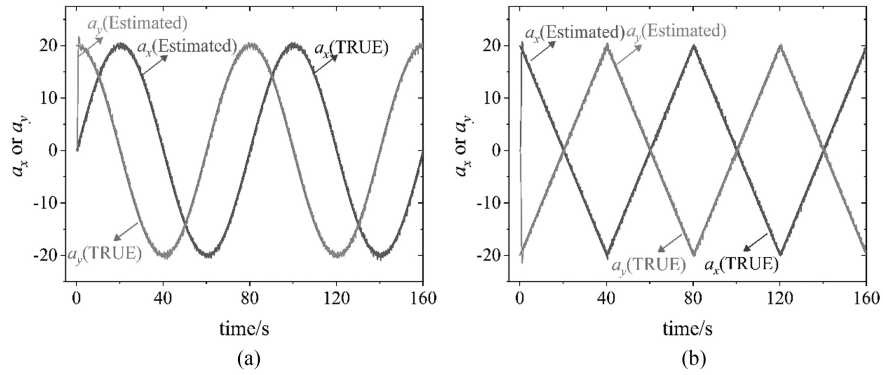

Figure 7. Estimation results of different types of unknown acceleration using OTSKF: (a) sinusoidal and (b) triangle.

m/s], [−14.72 m/s, 21.37 m/s] and [−4.05 m/s, 25.97 m/s] while the estimation error of V_y distributes in the ranges of [−5.11 m/s, 3.66 m/s], [−15.38 m/s, 12.03 m/s], [−18.50 m/s, 16.78 m/s] and [−3.96 m/s, 25.26 m/s]. And the error lasts for a relatively long time in each case. For OTSKF, its estimation results for velocity under different conditions are accurate. The estimation error only occurs at the moments when the acceleration changes. It can quickly reach zero. With the increase of $\boldsymbol{Q}$, the estimation error of velocity becomes lower, which is similar to the trajectory tracking and bias estimation results.

4.4 Target Tracking and Bias Estimation Using OTSKF with Different Types of Bias

Previous results demonstrate that under the low-noise condition, both the RTSKF and OTSKF can be used for the manoeuvring target tracking and its unknown bias estimation. When the noises increase, the OTSKF can resist the noises exhibiting high performance for simultaneous target tracking and bias estimation. In this section, different types of unknown bias are employed to investigate the flexibility of OTSKF in noisy environments. All initial guess values of state and bias are set as zero. To test the robustness, both the $\boldsymbol{Q}$ and $\boldsymbol{R}$ are set as $0.10\boldsymbol{I}$. The unknown acceleration sequences are set as sinusoidal and triangle with different initial values. The true values and estimation results of unknown acceleration are shown in Fig. 7.

For a sinusoidal unknown acceleration sequence, the initial values of true a_x and a_y are 0 and 20 m/s^2. Due to the reason that initial estimated value of them is set as zero, the estimated a_y quickly increases from zero to a high value near 20 m/s^2. In the following process, it is seen that estimated results can match the true value with a certain level of fluctuation which is caused by noises. It is an interesting phenomenon that the fluctuation intensity of estimated acceleration at 20 m/s^2 is slightly higher than that in other zones. This is caused by the changes in the true value herein. It is found that though the noise intensities are higher than in previous sections, the estimated results are still of high accuracy.

As for the triangle unknown acceleration sequence, the true values of a_x and a_y at the initial moment are 20 m/s^2 and −20 m/s^2, respectively. As the initial guess of estimated acceleration is zero, the estimated result quickly increases or decreases to 20 m/s^2 or −20 m/s^2 from zero. This tracking lasts for a very short period. Then, the estimated unknown bias agrees highly with the true acceleration.

Considering the previous sections, the OTSKF is demonstrated to have high performances to estimate different types of unknown bias. The state tracking results using OTSKF are shown in Fig. 8.

From the tracking results illustrated in Fig. 8, it is seen that the OTSKF can track the instantaneous movement of the manoeuvring target whatever the bias type is. The estimated velocity using OTSKF also highly coincided with the true velocity calculated from the model. To further demonstrate the accuracy, the estimation error distributions of the state are given as Fig. 9.

It is seen that the more than 99% tracking error of position is in the range from −0.1 m to 0.1 m. The tracking results of the y coordinate with triangle acceleration variation and the x coordinate with sinusoidal acceleration variation are higher than the other two. 99.999% error of them are in the aforementioned range. Compared with their coordinate of true position, the relative error is very small. As for the velocity estimation result, the $V_{x,\text{sinusoidal}}$ and $V_{y,\text{triangle}}$ are of higher accuracy, whose tracking errors are distributed in the range from −1 m/s to 1 m/s. For $V_{y,\text{sinusoidal}}$ and $V_{x,\text{triangle}}$, though there is some error of quite large values, more than 98.5% of them are in the range of [−1 m/s, 1 m/s]. That demonstrates the OTSKF can track the moving state of a manoeuvring target with different unknown accelerations.

5. Conclusion

The performances of RTSKF and OTSKF are compared for simultaneous target tracking and unknown bias estimation. The effects of different noisy parameters on the tracking performances are investigated. Additionally, the tracking results with different types of acceleration are obtained using OTSKF. Results demonstrate the RTSKF and OTSKF are feasible for the simultaneous estimation of the target state and unknown acceleration in a low-noise environment. When the intensity of measurement noises

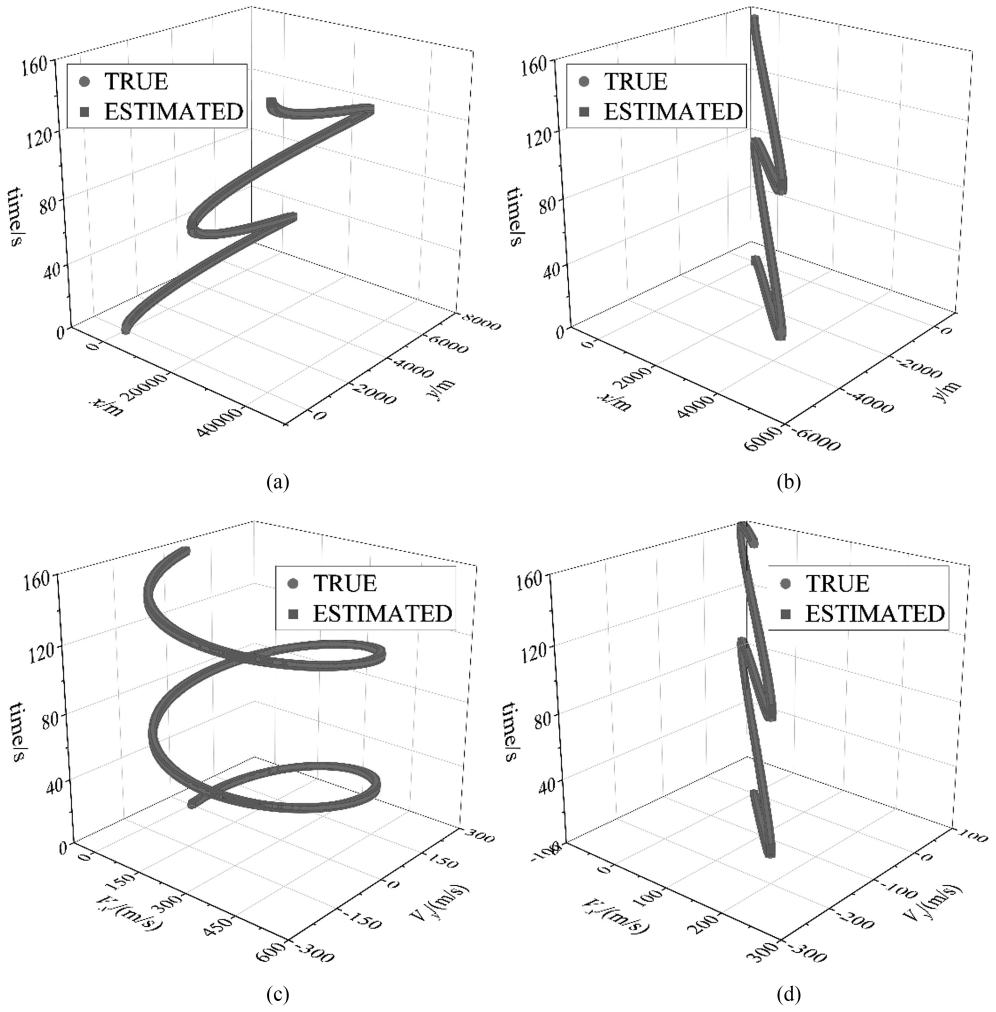

Figure 8. Manoeuvring target tracking results using OTSKF with different types of acceleration: (a) trajectory of sinusoidal bias; (b) trajectory of triangle bias; (c) velocity of sinusoidal bias; and (d) velocity estimation result.

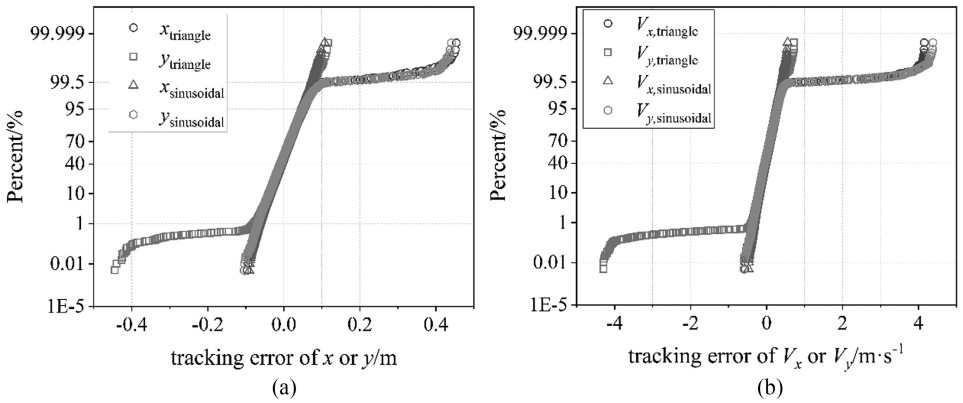

Figure 9. Tracking error distribution: (a) coordinate and (b) velocity.

increases, the estimation results of unknown bias and the state becomes worse whatever the RTSKF or OTSKF is used. The global error of OTSKF is lower than that of RTSKF under all conditions while RTSKF failed to track the target when $\boldsymbol{R} = 0.50\boldsymbol{I}$. When the noise of acceleration increases, the estimation errors of acceleration and velocity using RTSKF become worse while the trajectory tracking results have high accuracy. Under these conditions, OTSKF can be used to track the state and acceleration accurately. Increasing $\boldsymbol{Q}$ can improve the estimation precision due to the role of $\boldsymbol{Q}$ to modify the gain. OTSKF is demonstrated to have the high performance to estimate the moving state and track the trajectory with different types of unknown bias.

Acknowledgement

This work is supported by Research on Wireless Body Area Network Sensing Technology project of Science and Technology Research Program of Chongqing Education Commission of China (No: KJQN202103213).

References

[1] P. Dendorfer, A. Ošep, A. Milan, K. Schindler, D. Cremers, I. Reid, S. Roth, and L.L. Taixé, Motchallenge: A benchmark for single-camera multiple target tracking., *International Journal of Computer Vision, 129*, 2021, 845–881.

[2] J. Upadhyay, A. Rawat, and D. Deb, Multiple drone navigation and formation using selective target tracking-based computer vision, *Electronics-Switz, 10*, 2021, 2125.

[3] T.P. Nascimento and M. Saska, Position and attitude control of multi-rotor aerial vehicles: A survey, *Annual Reviews in Control, 48*, 2019, 129–146.

[4] Y. Liu, L. Yao, W. Xiong, T. Jing, and Z. Zhou, Ship target tracking based on a low-resolution optical satellite in geostationary orbit, *International Journal of Remote Sensing, 39*, 2018, 2991–3009.

[5] A. Jebelli, H. Chaoui, A. Mahabadi, and B. Dhillon, Tracking and mapping system for an underwater vehicle in real position using sonar system, *International Journal of Robotics and Automation, 37*(1), 2022, 124–134.

[6] M. Chiani, A. Giorgetti, and E. Paolini, Sensor radar for object tracking, *Proceedings of the IEEE, 106*, 2018, 1022–1041.

[7] J. Gu, T. Su, Q. Wang, X. Du, and M. Guizani, Multiple moving targets surveillance based on a cooperative network for multi-UAV, *IEEE Communications Magazine, 56*, 2018, 82–89.

[8] X. Sheng, L. Xu, and Z. Wang, A position-based explicit force control strategy based on online trajectory prediction, *International Journal of Robotics and Automation, 32*(1), 2017, 93–100.

[9] S. Zhao, Z. Zhu, C. Chen, Y. Du, X. Song, K. Yan, D. Jiang, L. Li, and A. Liu, Trajectory planning of redundant space manipulators for multi-tasks, *International Journal of Robotics and Automation, 38*(5), 2023, 344–351.

[10] A. Vitali, M. Battipede, and A. Lerro, Multi-objective and multi-phase 4D trajectory optimization for climate mitigation-oriented flight planning, *Aerospace, 8*, 2021, 395.

[11] J. Qi, H. Liao, Y. Xu, Z. Zhu, and C. You, Event-triggered attitude-tracking control for a cableless non-contact close-proximity formation satellite, *Aerospace, 9*, 2022, 138.

[12] P. Li, X. Wen, M. Zheng, H. Liu, D. Long, and Y. Lu, Discrete-time attitude tracking synchronization for swarms of spacecraft exploiting interference, *Aerospace, 9*, 2022, 134.

[13] S. Ziadi, M. Njah, M. Chtourou, and S. Charfi, PSO-DVSF2-mt: An optimized mobile robot motion planning approach for tracking moving targets, *International Journal of Robotics and Automation, 37*(5), 2022, 421–430.

[14] C. De, Q. Yan, J. Zhou, and Y. Du, An adaptive localisation method based on DBSCAN algorithm in mobile robot, *International Journal of Robotics and Automation, 38*(4), 2023, 323–333.

[15] G.S. Ting, S.A. Zekavat, and O. Abdelkhalik, An introduction to Kalman filtering implementation for localization and tracking applications, *Handbook of Position Location: Theory, Practice, and Advances*, 2nd ed.,, Hoboken, NJ, USA: Wiley, 2018, 143–195.

[16] F. Zheng and L. Shao, A winner-take-all strategy for improved object tracking, *IEEE Transactions on Image Processing, 27*, 2018, 4302–4313.

[17] Z. Pan, S. Liu, and W. Fu, A review of visual moving target tracking, *Multimedia Tools and Applications, 76*, 2017, 16989–17018.

[18] W. Jiaolong, W. Jihe, Z. Dexin, S. Xiaowei, and C. Guozhong, Kalman filtering through the feedback adaption of prior error covariance, *Signal Processing, 152*, 2018, 47–53.

[19] B. Ge, H. Zhang, L. Jiang, Z. Li, and M.M. Butt, Adaptive unscented Kalman filter for target tracking with unknown time-varying noise covariance, *Sensors-Basel, 19*, 2019, 1371.

[20] Y. Xu, K. Xu, J. Wan, Z. Xiong, and Y. Li, Research on particle filter tracking method based on Kalman filter, *Proc. IEEE Advanced Information Management,Communicates,Electronic and Automation Control Conference (IMCEC)*, 2018, 1564–1568.

[21] Y. Huang, Y. Zhang, P. Shi, Z. Wu, J. Qian, and J.A. Chambers, Robust Kalman filters based on Gaussian scale mixture distributions with application to target tracking, *IEEE Transactions on Systems, Man, and Cybernetics: Systems, 49*, 2017, 2082–2096.

[22] S.R. Jondhale and R.S. Deshpande, Kalman filtering framework-based real time target tracking in wireless sensor networks using generalized regression neural networks, *IEEE Sensors Journal, 19*, 2019, 224–233.

[23] H. Yang, J. Wang, Y. Miao, Y. Yang, Z. Zhao, Z. Wang, and Q. Sun, Combining spatio-temporal context and Kalman filtering for visual tracking, *Mathematics, 7*, 2019, 1059.

[24] U. Jung, M. Cho, J. Woo, and C. Kim, Trajectory-tracking controller design of rotorcraft using an adaptive incremental-backstepping approach, *Aerospace, 8*, 2021, 248.

[25] T. Ma, Q. Zhang, C. Chen, and S. Gao, Tracking of maneuvering star-convex extended target using modified adaptive extended Kalman filter, *IEEE Access, 8*, 2020, 214030–214038.

[26] P. Gu, Z. Jing, and L. Wu, Adaptive fading factor unscented Kalman filter with application to target tracking, *Aerospace Systems, 4*, 2021, 1–6.

[27] D. Wang, H. Zhang, and B. Ge, Adaptive unscented Kalman filter for target tacking with time-varying noise covariance based on multi-sensor information fusion, *Sensors, 21*, 2021, 5808.

[28] W. Zhou and J. Hou, A new adaptive high-order unscented Kalman filter for improving the accuracy and robustness of target tracking, *IEEE Access, 7*, 2019, 118484–118497.

[29] J. Yin, Z. Yang, and Y. Luo, Adaptive tracking method for non-cooperative continuously thrusting spacecraft, *Aerospace, 8*, 2021, 244.

[30] C. Liang, F. Wen, and Z. Wang, Trust-based distributed Kalman filtering for target tracking under malicious cyber attacks, *Information Fusion, 46*, 2019, 44–50.

[31] C.-C. Ji, P.C. Tuan, and H.Y. Jang, A recursive least-squares algorithm for on-line 1-D inverse heat conduction estimation, *International Journal of Heat and Mass Transfer, 40*, 1997, 2081–2096.

[32] M. LeBreux, M. Désilets, and M. Lacroix, Fast inverse prediction of phase change banks in high temperature furnaces with a Kalman filter coupled with a recursive least-square estimator, *International Journal of Heat and Mass Transfer, 53*, 2010, 5250–5260.

[33] H. Qi, S. Wen, Y. Wang, Y. Ren, L. Wei, and L. Ruan, Real-time reconstruction of the time-dependent heat flux and temperature distribution in participating media by using the Kalman filtering technique, *Applied Thermal Engineering, 157*, 2019, 113667.

[34] X. Wang, D. Zhang, and L. Zhang, Estimation of moving heat source for an instantaneous three-dimensional heat transfer system based on step-renewed Kalman filter, *International Journal of Heat and Mass Transfer, 163*, 2020, 120435.

[35] X. Wang, D. Zhang, L. Zhang, and C. Jiang, Real-time thermal states monitoring of absorber tube for parabolic trough solar collector with non-uniform solar flux, *International Journal of Energy Research, 42*, 2018, 707–719.

[36] C.-S. Hsieh and F.-C. Chen, Optimal solution of the two-stage Kalman estimator, *IEEE Transactions on Automatic Control, 44*, 1999, 194–199.

[37] J. Keller and M. Darouach, Optimal two-stage Kalman filter in the presence of random bias, *Automatica, 33*, 1997, 1745–1748.

[38] C.-S. Hsieh, Robust two-stage Kalman filters for systems with unknown inputs, *IEEE Transactions on Automatic Control, 45*, 2000, 2374–2378.

[39] S.L.V.A. Tummala and K.R. Inapakurthi, A two-stage Kalman filter for cyber-attack detection in automatic generation control system, *Journal of Modern Power Systems and Clean Energy, 10*, 2022, 50–59.

[40] J. Zhang, G. Welch, G. Bishop, and Z. Huang, A two-stage Kalman filter approach for robust and real-time power system state estimation, *IEEE Transactions on Sustainable Energy, 5*, 2014, 629–636.

[41] L. Xu, X.R. Li, and Z. Duan, Hybrid grid multiple-model estimation with application to maneuvering target tracking, *IEEE Transactions on Aerospace and Electronic Systems, 52*, 2016, 122–136.

[42] M.M. Rana, N. Halim, M.M. Rahamna, and A. Abdelhadi, Position and velocity estimations of 2D-moving object using Kalman filter: literature review, *Proc. 22nd International Conf. on Advanced Communication Technology (ICACT),* 541–544.

Biographies

Deng Hao was born in August, 1980. He is currently an Associate Professor with Chongqing Industry Polytechnic College. He received the master's degree from Chongqing University. He majors on automatic control, wireless sensor network, and image and graphics processing.